Available online at www.sciencedirect.com
SCIENCE DIRECT
Computers and Chemical Engineering 30 (2005) 147–157
Computers & Chemical Engineering
www.elsevier.com/locate/compchemeng

Development and application of linear process model in estimation and control of reactive distillation

Moshood J. Olanrewaju, Muhammad A. Al-Arfaj *

Department of Chemical Engineering, King Fahd University of Petroleum and Minerals, Dhahran 31261, Saudi Arabia

Received 29 September 2004; received in revised form 14 August 2005; accepted 18 August 2005
Available online 6 October 2005

Abstract

This paper presents a comprehensive formulation of a linearized state space process model for a generic two-reactant-two-product reactive distillation system. The development of the model requires the knowledge of the desired steady state design data, including liquid holdups and composition profiles. The application of the developed linear process model in composition estimation and control of the system is demonstrated. The effect of controller tuning on the performance of the estimator-based control system is explored. It is shown that effective controller tuning is necessary for a robust performance of a closed-loop reactive distillation system that relies on a state estimator. A robust linear state estimator can be developed and implemented in a feedback control system of a reactive distillation when the process can be approximated by a linear model.

Keywords: Reactive distillation; Linear state space model; State estimation and control

1. Introduction

The growing application of reactive distillation processes has necessitated a better understanding of its process dynamics and control. The classical problem of implementing a feedback control on a system is the means to provide the controllers the required feedback states. In practice, the use of online analyzer to measure the concentration in a reactive distillation column is unsatisfactory because of its economic implications. Besides, the large time delay between taking the sample and the output of the analyzer makes it difficult to be used in a feedback control system. Therefore, the use of a state estimator to provide the state estimates, when needed in the control system of a reactive distillation system, is an attractive alternative.

Recent publications on reactive distillation control emphasize the need to have the knowledge of internal composition profiles in order to design an effective control for reactive distillation (Al-Arfaj & Luyben, 2000, 2002a, 2002b, 2004; Bisowarno, Tian, & Tade, 2003; Wang, Wong, & Lee, 2003). Unless an excess of one of the reactants is incorporated in the process design, some detection of the inventory of one of the reactants in the column is required so that a feedback trim can balance the reaction stoichiometry (Al-Arfaj & Luyben, 2000).

Reactive distillation columns are generally being modeled by a set of highly nonlinear first order differential equations (Baur, Taylor, & Krishna, 2001; Kumar & Daoutidis, 1999; Roat, Downs, Vogel, & Doss, 1986; Taylor & Krishna, 2000). However, many model-based controllers use linear models because the linear models are easier to analyze and require less computational recourses than nonlinear models. Besides, most of the nonlinear systems often have the same general phase-plane behavior as the model linearized about the steady state condition when the system is close to that particular condition. Therefore, it is important to derive a suitable linearized dynamic model that when used in the model-based control applications could yield an effective and robust control system.

Few papers have emerged on the development of a linear model for a typical distillation column. Marquardt and Amrhein (1994) developed a linear distillation model for multivariable controller design of binary distillation columns. Their modeling idea draws on the wave propagation phenomena characterizing distillation column dynamics. The process nonlinearities were nicely averaged by using a 5th order linear model. Luyben (1987) derived a simple but effective method to determine suitable linear transfer functions for highly nonlinear distillation columns. He presented an effective design procedure that uses

* Corresponding author. Tel.: +966 3 860 1694; fax: +966 3 860 4234.
E-mail address: maarfaj@kfupm.edu.sa (M.A. Al-Arfaj).

0098-1354/$ – see front matter © 2005 Elsevier Ltd. All rights reserved.
doi:10.1016/j.compchemeng.2005.08.007

Nomenclature

A	reactant component
A	matrix of state variables for the linearized process model
B	reactant component
B	matrix of inputs for the linearized process model
C	product component
C	matrix of outputs for the linearized process model
d	disturbance variables' vector
E	matrix of the disturbance variables for the linearized process model
F_A	fresh feed flowrate of reactant A (kmol/s)
F_B	fresh feed flowrate of reactant B (kmol/s)
G	matrix of measurement noise
ΔH_v	heat of vaporization (cal/mol)
K	gain matrix
K_B	specific reaction rate of the reverse reaction (kmol s^{-1} $kmol^{-1}$)
K_c	Controller gain
K_F	specific reaction rate of the forward reaction (kmol s^{-1} $kmol^{-1}$)
KF	Kalman filter
L	liquid flowrate (kmol/s)
M_i	liquid holdup on stage i (kmol)
nf_1	first tray of reactive section (entrance of feed F_A)
nf_2	last tray of reactive section (entrance of feed F_B)
N	total number of stages including reboiler and reflux drum
P	column pressure
$R_{i,j}$	rate of production of component j on tray i (kmol/s)
T_i	temperature in stage i including reboiler (K)
U	input variables' vector
v	measurement noise
V_i	vapor flowrate on tray i (kmol/s)
V_S	vapor flowrate from the reboiler (kmol/s)
w	plant noise
$x_{bot,D}$	composition of D in the bottoms
$x_{dis,C}$	composition of C in the distillate
$x_{i,j}$	liquid mole fraction of component j on tray i
X	state vector of the variables
$\hat{X}$	state estimate vector
$X_{nf_1,A}$	composition of A in tray nf_1
$X_{nf_2,B}$	composition of B in tray nf_2
X_0	initial conditions of the plant model
X_0 err	initial condition error vector
Y	output vector
$\hat{Y}$	observation vector
Z	measured output vector
Z_a	composition of fresh feed F_A
Z_b	composition of fresh feed F_B

Greek letters

α_j	relative volatility of component j with respect to heavy component
δ_m	standard deviation of the measurement noise
δ_p	standard deviation of the plant noise
θ	lumped model parameters
λ	heat of reaction (cal/mol)

Astrom's method (relay feedback) to get critical gains and frequencies for each diagonal element of the plant transfer matrix. He concluded by emphasizing the effectiveness of the method in handling highly nonlinear column efficiently.

This study deals with the formulation of a linearized state space model, and demonstrates its applicability in an estimator-based control system of a generic reactive distillation. A linear state estimator is developed from a linear process model and implemented in a feedback control system of a reactive distillation. The function of the state estimators is to provide the required states for feedback. The robustness and reliability of a linear estimator at different operating conditions are examined by comparing the performance of an estimator based-control system to that of a system that assumes a perfect composition measurement. Section 2 presents a detailed nonlinear process model for a generic reactive distillation under study. Because the performance of a state estimator largely depends on the accuracy of the process model in which it is based on, Section 3 is devoted to developing a reliable linear process model for the system. The linearization of this nonlinear reactive distillation model is challenging because of the presence of reaction and separation in a single column. Complexity in its dynamics arises from the interaction of the reaction kinetics and distillation concept of vapor–liquid equilibrium in the system. The development of a linear state estimator is presented in Section 4. The performance of a dual-end composition control structure when all of the compositions are estimated by the linear estimator, and when the linearized process model is used to describe the reactive distillation process is investigated in Section 5.

2. Nonlinear process model

Various types of models, involving different levels of complexity, can be used to simulate the dynamics of reactive distillation column. In this work, we considered the simple and generic reactive distillation system studied by Al-Arfaj and Luyben (2000) as shown in Fig. 1. The system model captures the main features of the unit dynamics with simple vapor–liquid equilibrium, kinetics and physical properties. The reversible liquid-phase elementary reaction occurring in the reactive zone is

$$A + B \Leftrightarrow C + D \quad (1)$$

The assumptions considered are the following: constant liquid holdups; equimolar overflow except in the reaction zone where vapor boilup changes due to heat of reaction, which vaporizes some liquid on each tray; constant relative volatilities; fixed heat of reaction and vaporization; saturated liquid feed and reflux

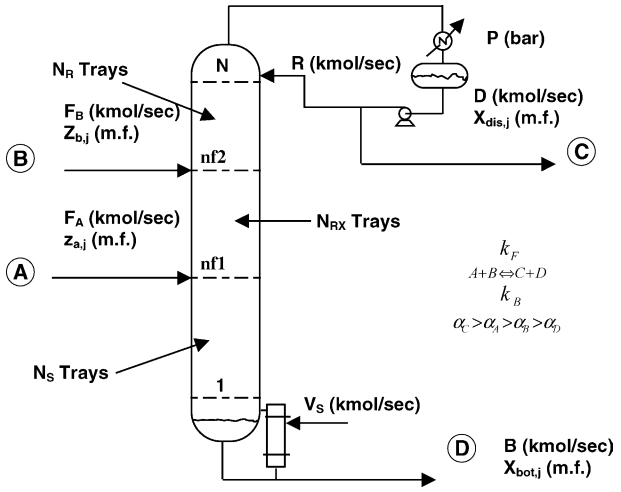

Fig. 1. Reactive distillation column.

flowrates. The column is considered to consist of five interconnected subsystems, which are: the reboiler, stripping section, reactive section, rectifying section and the condenser. The reactive section contains N_{RX} trays. The rectifying section contains N_R trays, and the stripping section below the reactive section contains N_S trays. Pure reactant A enters the column via the first tray (nf_1) of the reactive section and pure reactant B enters the column through the last reactive stage (nf_2). The reactive distillation column has total N stages (including a reboiler and total condenser) and is numbered from bottoms to the top.

The reactive distillation model is based on dynamic mass balance. To reduce the specificity to a certain chemical system and to reduce the model nonlinearities, the energy equations are neglected by assuming constant molar overflow except in the reactive zone. Because of this assumption, the vapor and liquid rates are constant through the stripping and rectifying sections. These rates change from tray to tray in the reactive zone because the heat of reaction vaporizes some liquid on each tray. Therefore, the nonlinear process models describing the system under study are presented as follows:

- Reboiler ($i = 1$):

$$\frac{dx_{1,j}}{dt} = \frac{L_2(x_{2,j} - x_{1,j}) + V_S(x_{1,j} - y_{1,j})}{M_1}, \quad j = 1, \ldots, N_c \tag{2}$$

- Stripping section ($2 \le i \le N_S + 1$):

$$\frac{dx_{i,j}}{dt} = \frac{L_{i+1}(x_{i+1,j} - x_{i,j}) + V_S(y_{i-1,j} - y_{i,j})}{M_i}, \quad j = 1, \ldots, N_c \tag{3}$$

- Reactive section ($nf_1 \le i \le nf_2$), $F_i = 0$ except at $i = nf_1, nf_2$:

$$\frac{dx_{i,j}}{dt} = \frac{L_{i+1}(x_{i+1,j} - x_{i,j}) + V_{i-1}(y_{i-1,j} - x_{i,j}) + V_i(x_{i,j} - y_{i,j}) + R_{i,j} + F_i(Z_{i,j} - x_{i,j})}{M_i}, \quad j = 1, \ldots, N_c \tag{4}$$

- Rectifying section ($nf_2 + 1 \le i \le N_S + N_{RX}$):

$$\frac{dx_{i,j}}{dt} = \frac{L_{i+1}(x_{i+1,j} - x_{i,j}) + V_n(y_{i-1,j} - y_{i,j})}{M_i}, \quad j = 1, \ldots, N_c \tag{5}$$

- Condenser:

$$\frac{dx_{N,j}}{dt} = \frac{V_n(y_{N-1,j} - x_{N,j})}{M_N}, \quad j = 1, \ldots, N_c \tag{6}$$

The vapor and liquid flowrates on tray i of the reactive section are given as:

$$V_i = V_S + \frac{\lambda}{\Delta H_v} \sum_{k=1}^{i-N_S-1} R_{N_S+1+k,j} \tag{7}$$

$$L_i = L_{i-1} + \frac{\lambda}{\Delta H_v} \sum_{k=1}^{i-N_S-1} R_{N_S+1+k,j} \tag{8}$$

The reaction rate (kmol/s) of component j on tray i is given as:

$$R_{i,j} = M_i(k_{F,i}x_{i,A}x_{i,B} - k_{B,i}x_{i,C}x_{i,D}) \tag{9}$$

The forward and backward specific reaction rates (kmol s^{-1} $kmol^{-1}$) on tray i are:

$$k_{F,i} = a_F\, e^{-E_F/RT_i} \tag{10}$$

$$k_{B,i} = a_B\, e^{-E_B/RT_i} \tag{11}$$

where a_F and a_B are the pre-exponential factors, E_F and E_B are the activation energies, and T_i is the absolute temperature on tray i. The vapor–liquid equilibrium equations are:

$$y_{i,j} = \frac{\alpha_j x_{i,j}}{\sum_{k=1}^{N_c} \alpha_k x_{i,k}} \tag{12}$$

$$T_i = \frac{B_{vp,1}}{A_{vp,1} - \ln(\alpha_1 P / \sum_{k=1}^{N_c} \alpha_k x_{i,k})} \tag{13}$$

Eqs. (2)–(13) can be put in a more compact vector form to give a nonlinear state space model of a reactive distillation:

$$\frac{dX(t)}{dt} = f(X(t), U(t), d(t); \theta) \tag{14}$$

$$Y = h(X(t); \theta) \tag{15}$$

where "X" is a vector of state variables, which are liquid mole fractions. "U" is a vector of input variables, which are vapor boilup (V_S) from the reboiler and reflux flowrate (R) from condenser. "d" is a vector of measurable disturbance variables, which are the fresh feed flowrates of reactants A and B with their feed compositions. "Y" is a vector of measurable outputs, which can be either the column temperatures or the products compositions. θ is the system constant parameters, such as component relative volatilities, reaction kinetics data and the column pressure.

3. Linear process model

The linearization of the nonlinear equations (14) and (15) is carried out by using the Taylor series expansion. This implies that these sets of nonlinear equations are approximated by a truncated Taylor series approximation around the steady state operating conditions. Although, the Taylor series-based linearization method is a well-established technique, however, the most challenging aspect of its application is the formation of the resulting Jacobian matrices of the multivariable states for a coupled and a highly nonlinear dynamic model (Wolbert, Joulia, Koehret, & Biegler, 1994).

3.1. Linearized state space model formulation

If the nonlinear function $f(x)$ from Eq. (14) and the output nonlinear equation (15) is given as:

$$f(x) = \begin{bmatrix} f_1(x_{1,1}, x_{2,1}, ..., x_{N,4}, u_1, u_2, ..., u_p, d_1, d_2, ..., d_q; \theta) \\ f_2(x_{1,1}, x_{2,1}, ..., x_{N,4}, u_1, u_2, ..., u_p, d_1, d_2, ..., d_q; \theta) \\ \vdots \\ f_{5N}(x_{1,1}, x_{2,1}, ..., x_{N,4}, u_1, u_2, ..., u_p, d_1, d_2, ..., d_q; \theta) \end{bmatrix} \tag{16}$$

$$Y(x) = \begin{bmatrix} h_1(x_{1,1}, x_{2,1}, ..., x_{N,4}; \theta) \\ h_2(x_{1,1}, x_{2,1}, ..., x_{N,4}; \theta) \\ \vdots \\ h_q(x_{1,1}, x_{2,1}, ..., x_{N,4}; \theta) \end{bmatrix} \tag{17}$$

then, the linearization version of the nonlinear functions is obtained by taking the first two terms of the Taylor series:

$$f(X) = f(\bar{X}, \bar{U}, d; \theta) + \frac{\partial f}{\partial X}(X - \bar{X}) + \frac{\partial f}{\partial U}(U - \bar{U}) + \frac{\partial f}{\partial d}(d - \bar{d}) \tag{18}$$

$$Y(X) = h(\bar{X}; \theta) + \frac{\partial h}{\partial X}(X - \bar{X}) \tag{19}$$

In Eq. (18), the derivative of $f(X)$ is a derivative of a $4N \times 1$ vector with respect to a $4N \times 1$ state vector, $p \times 1$ input vector and $m \times 1$ disturbance vector. This results in:

1. $4N \times 4N$ Jacobian matrix "A" whose (i,j)th element is $\partial f_i/\partial x_j$;
2. $4N \times p$ input matrix "B" with $\partial f_i/\partial u_j$ coefficient as its element;
3. $4N \times m$ disturbance matrix "E" with (i,j)th element as $\partial f_i/\partial d_j$;
4. $q \times 4N$ output matrix "C" with $\partial h_i/\partial x_j$ coefficient as its element.

The steady state condition corresponds to $f(\bar{X}, \bar{U}, d; \theta) = 0$ and, $h(\bar{X}; \theta) = 0$ and all of the matrices elements are evaluated at steady state values. Therefore, the deviation variables arise naturally out of the Taylor series expansion, and the linearized state space model is given as:

$$\frac{dX}{dt} = AX(t) + BU(t) + Ed(t) \tag{20}$$

$$Y = CX(t) \tag{21}$$

The development of a reliable linearized process model depends strongly on the availability of a stable steady state conditions at the required operating specifications. The kinetic, physical, and vapor–liquid equilibrium parameters for our system are obtained from the work of Luyben (2000) and are summarized in Table 1, while the steady state design data are presented in Table 2.

3.2. Model linearity

A linear system is one that satisfies both homogeneity and additivity property. Before the applicability of a linearized model is assessed, it is important to demonstrate that this principle of superposition is satisfied. The linearity of the proposed model is tested by exciting the system with various magnitudes of step input changes. For illustration purposes, ±2% and ±4% step changes in feed flowrate of reactant B (F_B) are made, while the feed flowrate of reactant A (F_A), vapor boil up and the reflux flowrate are kept constant. Fig. 2 shows the openloop dynamic responses of the system to changes in the feed rate of reactant B. The symmetric nature of the output responses, with the same speed of response, is a clear indication of model linearity. Step

Table 1
Kinetic and physical properties

Activation energy (cal/mol)	
Forward	30000
Backward	40000
Specific reaction rate at 366 K (kmol s^{-1} kmol^{-1})	
Forward	0.008
Backward	0.004
Heat of reaction (cal/mol)	−10000
Heat of vaporization (cal/mol)	6944
Relative volatility	
α_C	8
α_A	4
α_B	2
α_D	1

Component	Vapor pressure	
	A_{vp}	B_{vp}
A	12.34	3862
B	11.45	3862
C	13.04	3862
D	10.96	3862

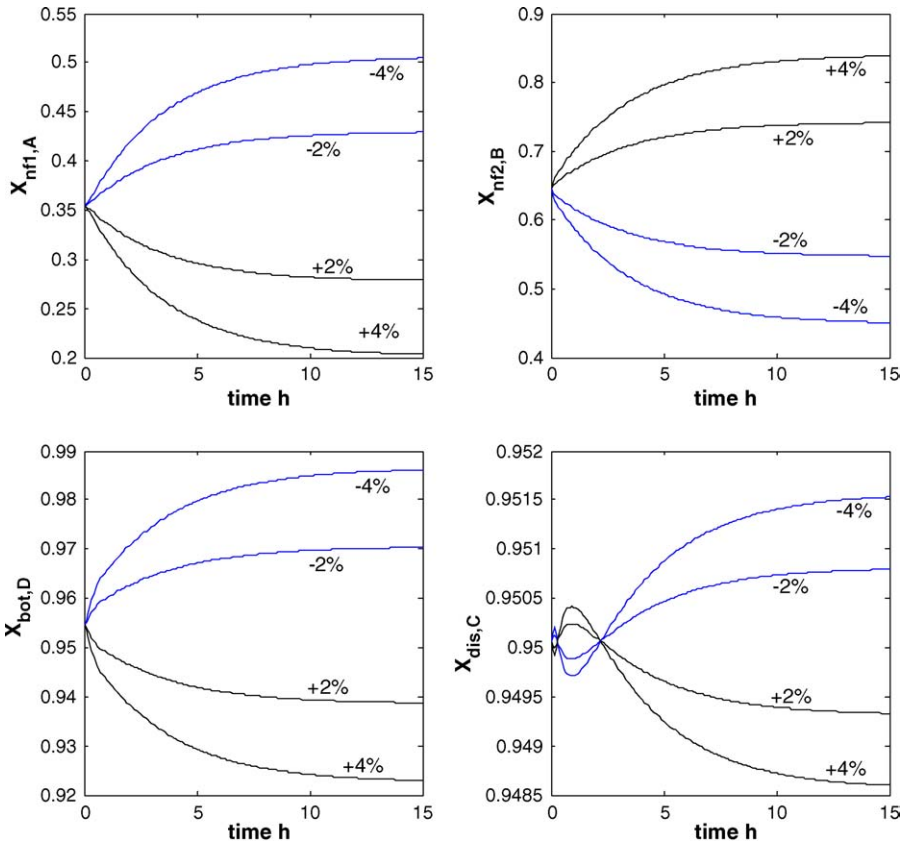

Fig. 2. Dynamic composition profile of the reactant A on the tray nf_1, the reactant B on the tray nf_2, the product C in the distillate and the product D in the bottoms with ±2 and ±4% change in F_B.

changes in the feed flowrate of reactant B from the steady state value changes the proportion of the of reactants concentration in the reactive zone and consequently, the amount of the impurity in the product streams. Our study on the dynamic comparison of nonlinear and linear models shows that an analogous dynamic behavior is observed around the base steady state. A linear model can approximate the nonlinear model well when the magnitude of input change is small. The deviation between the two models increases with increase in the magnitude of input change.

Table 2
Steady state design conditions

Variables	Steady state values
Column specifications	
Pressure (bar)	9
Stripping section	7
Reactive section	6
Rectifying section	7
Flowrates (kmol/s)	
V_S	0.0285
R	0.0331
D	0.0126
B	0.0126
$F_A = F_B$	0.0126
X_{dis}	
A	0.0467
B	0.0033
C	0.9501
D	0.0000
X_{bot}	
A	0.0009
B	0.0445
C	0.0000
D	0.9545

3.3. System stability

Systems are generally designed to either process some signals or perform some tasks. Thus, if a system is unstable, it may grow unbounded, saturate and disintegrate when a signal, no matter how small, is applied. Therefore, stability is a basic requirement for all systems. Since our system response is typical of zero-state, its stability can easily be verified using bounded-input–bounded-output (BIBO) stability criteria. A multivariable process is openloop stable if and only if all the eigenvalues of matrix A have negative real parts (Chen, 1999). Table 3 shows the eigenvalues of matrix A for a linearized reactive distillation system with 20 trays, a reboiler and a condenser (i.e., $N = 22$). As shown in Table 3, the system is stable since all of the eigenvalues have negative real parts.

4. Linear state estimator and control system

4.1. Linear state estimator

A linear Kalman filter is developed using the linearized process model. Because all systems are subject to noise, which

Table 3
Eigenvalues of matrix A ($4N \times 4N$), $N = 22$, column configuration: 7/6/7 with reboiler and condenser

Eigenvalues of matrix A ($4N \times 4N$), $N = 22$			
−0.5221	−0.1592 + 0.0098i	−0.0747 + 0.0083i	−0.0323 + 0.0187i
−0.4483	−0.1592 − 0.0098i	−0.0747 + 0.0083i	−0.0458
−0.3935	−0.1571	−0.0728	−0.0267 + 0.0174i
−0.3894	−0.1506	−0.0685 + 0.0011i	−0.0267 − 0.0174i
−0.3564	−0.1267 + 0.0556i	−0.0685 − 0.0011i	−0.0398
−0.3170	−0.1267 − 0.0556i	−0.0588 + 0.0075i	−0.0365 + 0.0017i
−0.3016	−0.1086 + 0.0429i	−0.0588 − 0.0075i	−0.0365 − 0.0017i
−0.2898	−0.1086 + 0.0429i	−0.0595 + 0.0027i	−0.0365
−0.2502	−0.1308	−0.0595 − 0.0027i	−0.0226 + 0.0152i
−0.2347 + 0.0496i	−0.1285	−0.0554 + 0.0108i	−0.0226 − 0.0152i
−0.2347 − 0.0496i	−0.1210 + 0.0130i	−0.0554 − 0.0108i	−0.0289
−0.2369 + 0.0285i	−0.1210 − 0.0130i	−0.0515 + 0.0143i	−0.0166 + 0.0119i
−0.2369 − 0.0285i	−0.1222 + 0.0029i	−0.0515 − 0.0143	−0.0166 − 0.0119i
−0.2016 + 0.0562i	−0.1222 − 0.0029i	−0.0471 + 0.0167i	−0.0249
−0.2016 + 0.0562i	−0.1027	−0.0471 − 0.0167i	−0.0214
−0.2064	−0.0935 + 0.0215i	−0.0547	−0.0153 + 0.0063i
−0.1792 + 0.0695i	−0.0935 − 0.0215i	−0.0426 + 0.0187i	−0.0153 − 0.0063i
−0.1792 − 0.0695i	−0.0973	−0.0426 − 0.0187i	−0.0181
−0.1941	−0.0868 + 0.0117i	−0.0530	−0.0169
−0.1562 + 0.0633i	−0.0868 − 0.0117i	−0.0370 + 0.0193i	−0.0134
−0.1562 − 0.0633	−0.0836	−0.0370 − 0.0193i	−0.0100 + 0.0050i
−0.1619	−0.0791	−0.0323 + 0.0187i	−0.0100 − 0.0050i

could be in the form of unmodeled input effects, unmodeled dynamics, or undesired signals that act as inputs to the system at different points, the linear Kalman filter is developed from a noise-corrupted process model. Therefore, the linear state space model is described as

$$\frac{\mathrm{d}X(t)}{\mathrm{d}t} = AX(t) + BU(t) + Ed(t) + w(t) \tag{22}$$

$$Z = CX(t) + v(t) \tag{23}$$

where the $w(t)$ and $v(t)$ are vectors of the plant noise and measurement noise respectively, and Z is a vector of noise-contaminated measurement data. The relevant equations describing a linear estimator are therefore summarized as follows:

$$\hat{X}(0) = X_0 + X_0\,\mathrm{err} \tag{24}$$

$$Y = C\hat{X}(t) \tag{25}$$

$$\dot{\hat{X}}(t) = A\hat{X}(t) + BU(t) + Ed(t) + K[Z(X(t)) - Y(\hat{X}(t))] \tag{26}$$

where X_0 err is a vector of the initial condition error.

A Kalman filter (KF) algorithm (Sorenson, 1985) utilizing a steady state Riccati equation is used to evaluate the filter gain K. The KF design procedure is summarized as follows:

(i) Initialize R and Q, where Q is the covariance matrix of the measurement error and R is the covariance matrix of the process noise.
(ii) Obtain the covariance matrix P by solving the steady state Riccati equation as

$$AP + PA^{\mathrm{T}} - PC^{\mathrm{T}}R^{-1}CP + Q = 0 \tag{27}$$

(iii) Compute the gain matrix K

$$K = PC^{\mathrm{T}}R^{-1} \tag{28}$$

4.1.1. Observability

In order to design a state estimator, it is necessary that the system is observable. A linear system is observable if the matrix

$$O = [\,C \quad CA \quad CA^2 \quad \ldots \quad CA^{4N-1}\,] \tag{29}$$

is a full column rank (i.e. of rank $4N$). O is termed the observability matrix. Simulation studies on our system by utilizing the observability condition of Eq. (29) show that using not less than $N/2$ temperature measurements uniformly distributed in the column is a sufficient condition to observe all of the components liquid compositions of reactive distillation under study.

4.2. Control system

We considered a dual-end composition control structure shown in Fig. 3, where the purities of both products are controlled. In the distillate product, the composition of component C ($\hat{x}_{\mathrm{dis,C}}$) is controlled by manipulating the reflux flowrate. In the bottoms, the composition of component D ($\hat{x}_{\mathrm{bot,D}}$) is controlled by manipulating the vapor boilup. The reflux-drum level is controlled by the distillate flowrate, while the bottoms level is controlled by manipulating the bottoms flowrate. To balance the reaction feeds stoichiometry, the concentration of reactant A on the tray nf_1 ($\hat{x}_{\mathrm{nf}_1,\mathrm{A}}$) is measured and controlled by manipulating the feed flowrate of component A. The internal composition controller is P-only with controller gain of 0.95. The remaining composition controllers for product purities are PI. The tuning method for these controllers is discussed in Section 4.3. All of the control valves are designed to be half open at the initial

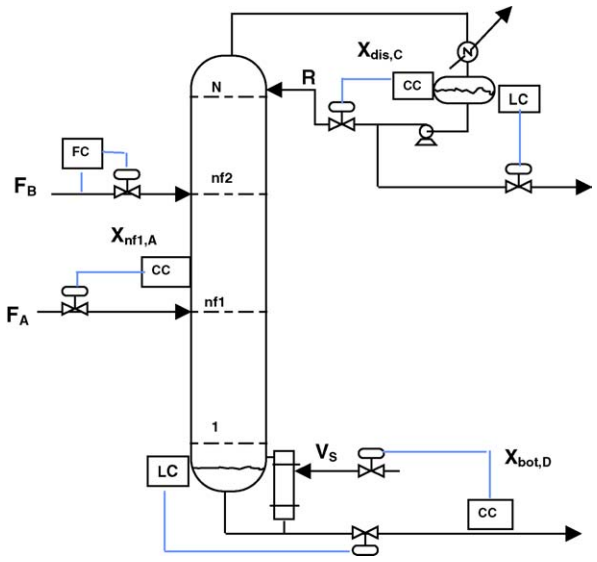

Fig. 3. Dual-end composition control structure.

steady state. Therefore, all of the manipulated variables cannot increase more than twice their steady state values.

The most fundamental concept in this control system is the use of the estimator to provide the controllers the required states for feedback control. Therefore, Eqs. (22)–(26) can be combined to form the estimator-based control system:

$$\begin{bmatrix} \dot{X} \\ \dot{\hat{X}} \end{bmatrix} = \begin{bmatrix} A & \\ KC & A - KC \end{bmatrix} \begin{bmatrix} X \\ \hat{X} \end{bmatrix} + \begin{bmatrix} B \\ B \end{bmatrix} U + \begin{bmatrix} E \\ E \end{bmatrix} d \quad (30)$$

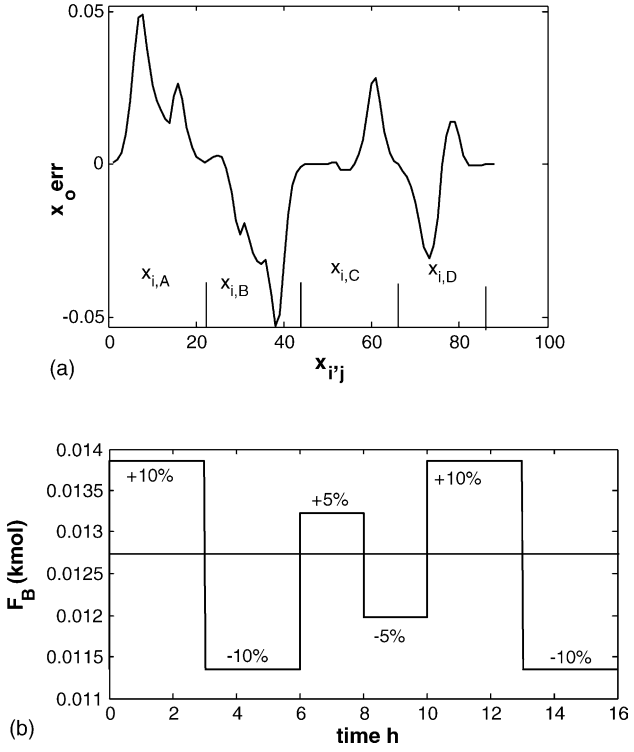

Fig. 4. (a) The base initial condition error; (b) a pseudo-rectangular random sequence (PRRS) forcing function on F_B.

$$\begin{bmatrix} Z \\ \hat{Y} \end{bmatrix} = [\,C \quad 0\,] \begin{bmatrix} X \\ \hat{X} \end{bmatrix} + [\,G \quad 0\,]v \quad (31)$$

The state estimator has three input variable vectors, which are

$$U = [V_S, F_A, R]^T \quad (32)$$

$$d = [Z_{a,j}, Z_{b,j}, F_B]^T \quad (33)$$

$$Z = [T_1, T_3, T_5, T_7, T_9, T_{11}, T_{13}, T_{15}, T_{17}, T_{19}, T_{21}]^T \quad (34)$$

and all of the three required controlled variables (i.e., $\hat{x}_{nf_1,A}$, $\hat{x}_{bot,D}$, $\hat{x}_{dis,C}$) are estimated by the state estimator and fed into the controllers for necessary actions.

4.3. Controllers tuning

Effective controllers tuning has a significant impact on the performance of the estimator-based control system. In order to illustrate this, the loops of the PI controllers are tuned by conducting a relay-feedback test (Luyben, 1987) to find ultimate gains and frequencies. Two different methods are studied to obtain the controllers settings:

1. The Ziegler–Nichols (Z–N) tuning;
2. The Tyreus–Luyben (TL) tuning (Tyreus & Luyben, 1992).

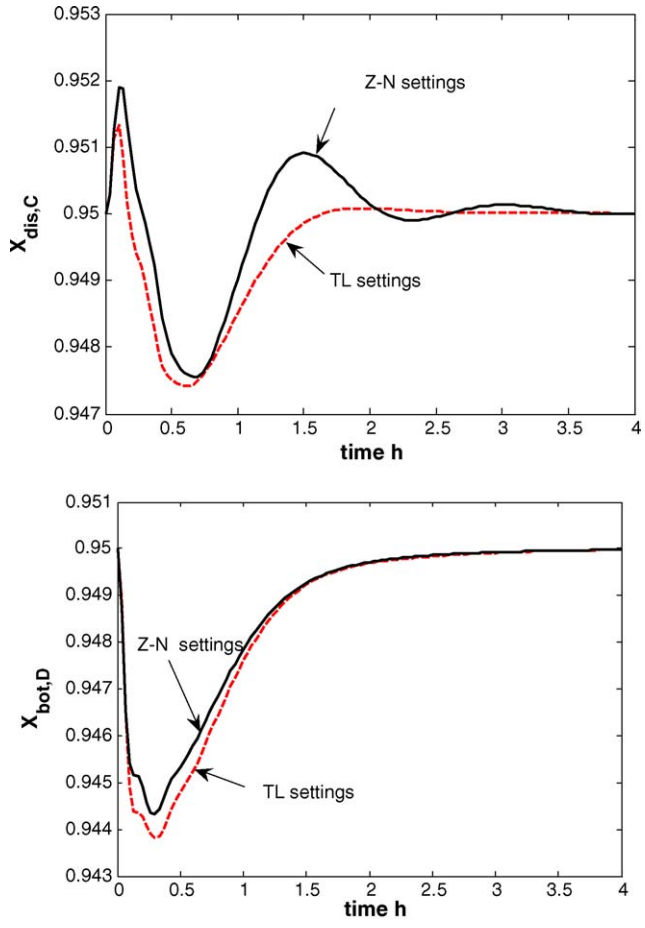

Fig. 5. Effect of tuning methods on the performance of estimator-based controllers with a disturbance of 10% F_B: (—) TL tuning; (- - -) Z–N tuning.

Table 4
Composition controllers tuning parameters

	Controlled variable		
	$x_{dis,C}$ (R,[a] PI[b])	$x_{bot,D}$ (V_S,[a] PI[b])	x_{nf_1}, A (F_A,[a] P-only[b])
Relay-feedback test			
K_u	9.73	12.23	
P_u (min)	11.36	7.27	
TL tuning constant			
K_c	3.04	3.82	0.95
τ_i (min)	24.99	16.00	
Z–N tuning constant			
K_c	4.42	5.56	0.95
τ_i (min)	9.47	6.05	

[a] Manipulated variable.
[b] Controller type.

To show the difference of these tuning methods on the performance of our system, fresh feed flowrate of reactant B (F_B) is increased by 10%. For a state estimator design purposes, both the plant noise (w) and measurement (v) noise is assumed to be white with the standard deviation of 1 and 10% respectively. The base initial condition error (X_0 err) used in the linear estimator simulation is shown in Fig. 4(a). The setpoint of products C and D in the distillate and bottoms is set to 95 mol%.

Fig. 5 compares the performance of the estimator-based control system under both TL and Z–N tuning methods. Both the TL and Z–N tuning methods give a good control performance. The Z–N settings produce a more aggressive and oscillatory responses while the TL settings provide more conservative and robust performance. Table 4 summarizes the tuning parameters for the two methods used.

To further investigate the effect of controller tuning on the control performance of our system, different values of controller gains are tested. This time, we considered only the TL settings, whereby the base controller gains (see Table 4) are reduced by half ($K_c/2$), and increase by a factor of 2 ($2K_c$) and 3 ($3K_c$). The system response for a 10% increase in F_B under the different controller gains ($K_c/2$, $2K_c$ and $3K_c$) is shown in Fig. 6. The results demonstrate that the control performance can be improved by increasing the gain values obtained from TL settings by a factor of 2. Thereafter, increasing these gain values (i.e., by a factor of 3) makes little difference. On the other hand, decreasing the gain values (from that suggested by TL settings) by half will impact the control performance and result into a poor system response. This shows the importance of using well-tuned controllers to obtain robust control performance.

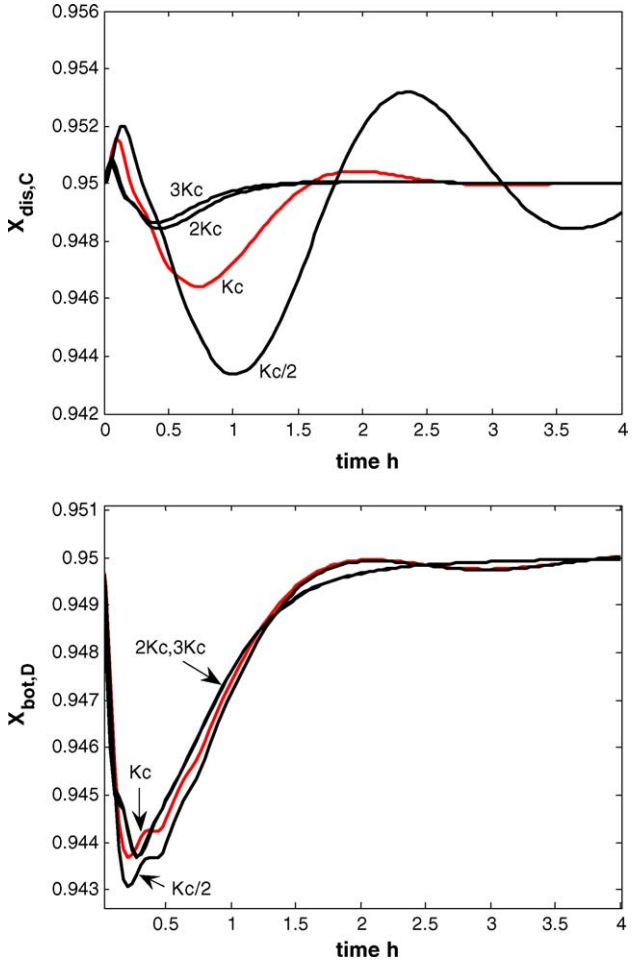

Fig. 6. Control performance at different values of controller gains with a disturbance of 10% F_B. K_c is the gain obtained from TL tuning.

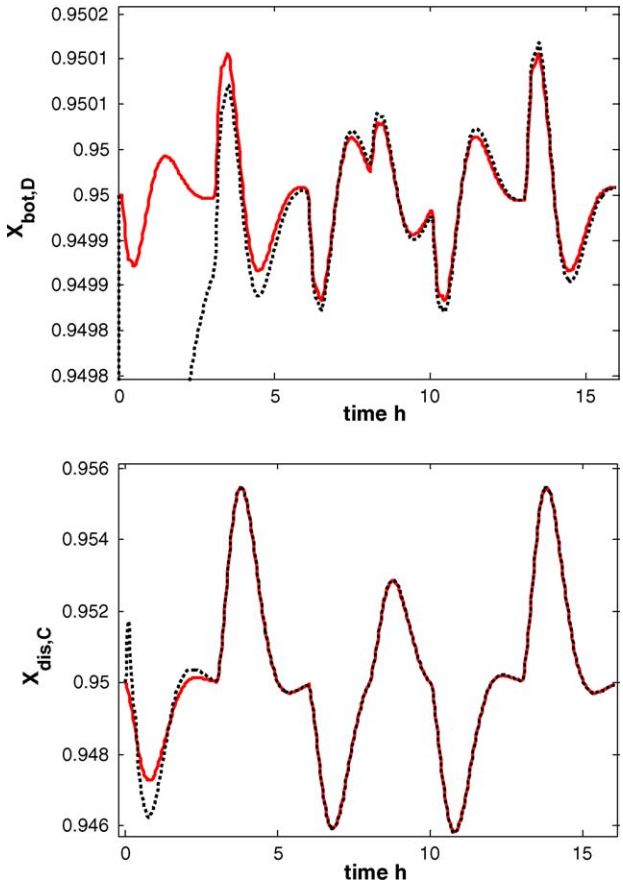

Fig. 7. Control performance with a PRRS forcing function on F_B. The base initial condition errors, $\delta_m = 10\%$ and $\delta_p = 1\%$ are used for KF design. (—) measured states for feedback; (- - -) estimated states for feedback.

5. Performance

The linear Kalman filter is implemented in the control system where the linearized model is used to represent the process model. The function of a linear Kalman filter is to estimate the three compositions (i.e., $\hat{x}_{nf_1,A}$, $\hat{x}_{bot,D}$, $\hat{x}_{dis,C}$) that are needed in the control structure. The performance of this control structure is compared to the same control structure when all of the three compositions are measured using online analyzer. Following the discussion in Section 4.3 and for the remaining simulation studies, controllers gains are increased by a factor of 2 over those suggested by the TL settings. The liquid holdup of 1 kmol is assumed in all of the stages, while the steady state conditions presented in Table 1 is used as the initial conditions for the real process model.

5.1. Disturbance rejection and setpoint tracking

Two different types of changes in the operating variables are investigated: a pseudo-rectangular random sequence (PRRS) forcing function on F_B as shown in Fig. 4(b), and the setpoint changes in products concentration. Fig. 7 compares the responses of the controlled variables (i.e., $x_{dis,C}$ and $x_{bot,D}$) of the system that relies on the state estimator to that when a perfect and direct composition measurement is assumed. The disturbance is a PRRS on F_B. These results show that a good control performance can be achieved when system controllers depend on the estimated states for decision-makings.

The effect of the large estimated errors at the startup can be noticed from the poor tracking of the reference setpoint at the early stage of operation. This is because the estimator takes some times to overcome the effect of the present initial conditions error, plant noise and measurement noise. As soon as the estimator adjusts for those factors, the estimator makes a better estimates and the control performance of the system improves accordingly. Note that the poor performance of the estimator at the early stage of the operation is more pronounced in the performance of the $x_{bot,D}$ composition controller because of the highest system inertia in the bottoms.

Fig. 8 suggests that setpoint changes in the product purities can be handled by a control system that uses the state estimator. The products purity is changed from 95 to 93% and to 97%. The estimator-based system is able to track asymptotically the new reference points, and suppress the effect of the present base initial conditions error, plant and measurement noise.

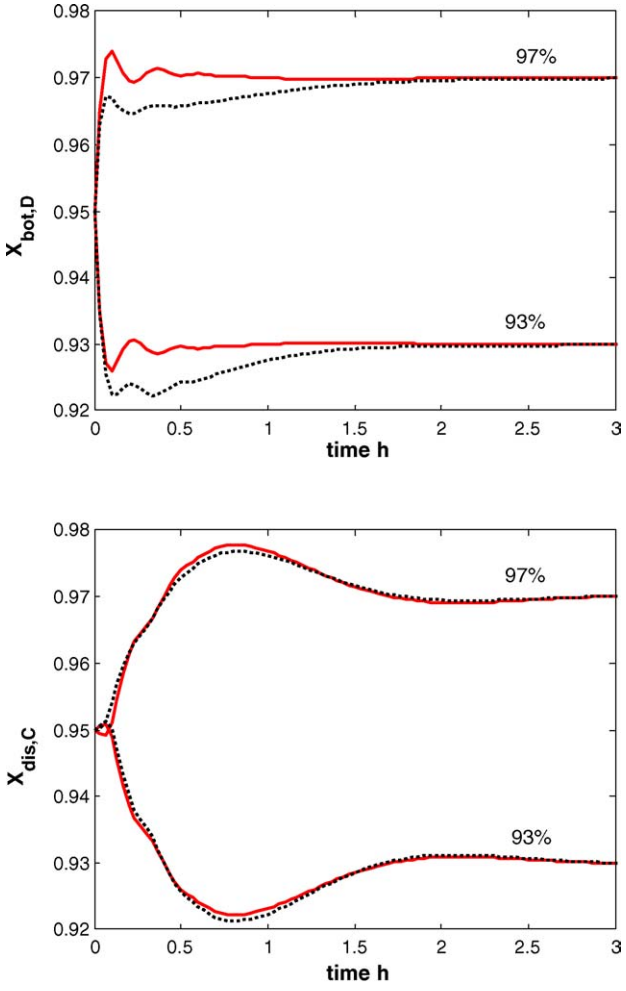

Fig. 8. Control performance to setpoint changes: $x_{bot,D}$ and $x_{dis,C}$ from 95 to 93% and to 97%; the base initial conditions error, $\delta_m = 10\%$ and $\delta_p = 1\%$ are used for KF design; (—) measured states for feedback; (- - -) estimated states for feedback.

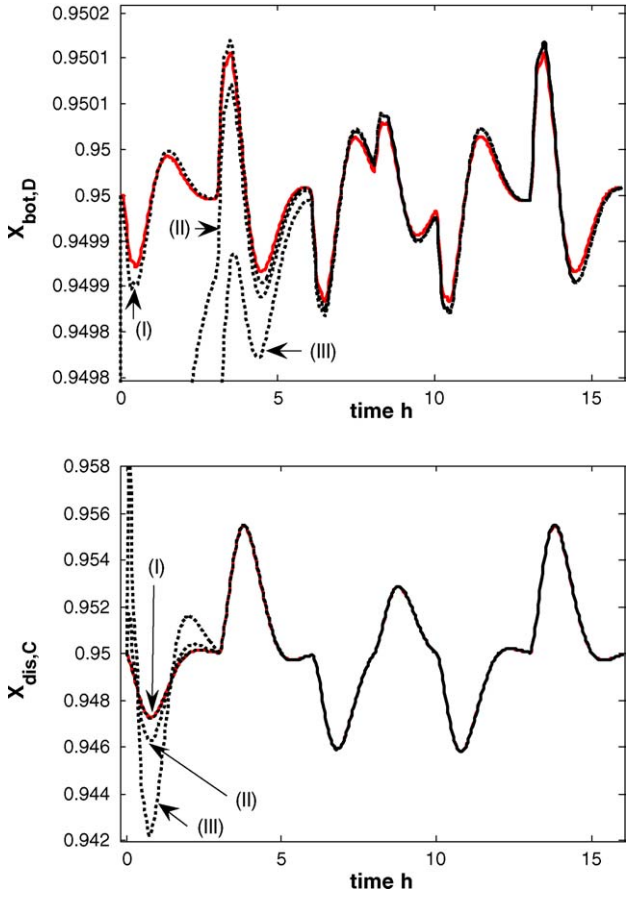

Fig. 9. Effect of erroneous initial conditions on the control performance with a PRRS forcing function on F_B: (I) no error; (II) base error (X_0 err); (III) $5X_0$ err, $\delta_m = 10\%$ and $\delta_p = 1\%$ are used for KF design, (—) measured states for feedback; (- - -) estimated states for feedback.

5.2. Initial conditions error

Because the exact steady state condition of a system is often not known, the developed state estimator should be able to start with approximate initial conditions. To investigate the effect of erroneous initial conditions on the quality of information obtained from a linear state estimator, and in turn, the performance of the control system that relies on such estimator, three different set of initial conditions are used to simulate the estimator. The first set of the initial conditions is the same as that of a real system (i.e., no error). The second is the base initial conditions used in the previous section (see Fig. 4(a)), while the third set is five times the magnitude of the base initial conditions errors ($5X_0$ err).

Fig. 9 shows the control performance of the system when the estimator is simulated with the three set of initial conditions. The results demonstrate that an excellent control performance of the estimator-based system can be achieved when accurate information of the initial steady state conditions is available. The responses of the system when the third set of initial conditions is used suggest that the state estimator is robust to initial conditions error. However, the implication is that it takes the controllers much more time to achieve the control specifications. Therefore, a reasonable set of initial conditions close enough to the base steady state conditions is required to simulate the state estimator for a robust control performance.

5.3. Plant-model mismatch

This section investigates control performance of a system when the state estimator design is based upon erroneous noise models. An incorrect plant description and/or errors in the some systems parameters of a process model will have a significant impact on the performance of a state estimator designed from such a model. To investigate this, an error of 0.1 is introduced to the relative volatilities of the components. This implies that the sensitivities matrices A, B, C and E of the state estimator model will not be the same as those in the linear process model. Fig. 10 shows the effect of erroneous relative volatilities on the control performance of the system that depends on a state estimator. The control performance is generally poor. An inaccurate vapor–liquid equilibrium has a more severe effect on the composition controller for the product D purity because of the highest system inertia in the bottoms. Therefore, for a successful implementation and application of a state estimator in a reactive distillation control, more effort is needed to obtain an accurate process model.

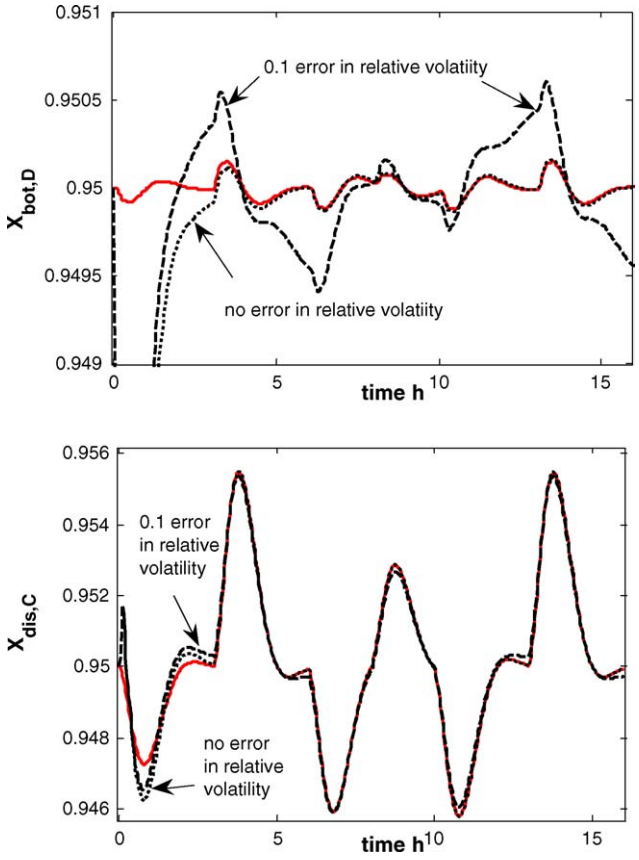

Fig. 10. Effect of erroneous relative volatility on control performance with a PRRS forcing function on F_B: the base initial conditions error, $\delta_m = 10\%$ and $\delta_p = 1\%$ are used for KF design; (—) measured states for feedback; (- - -) estimated states for feedback.

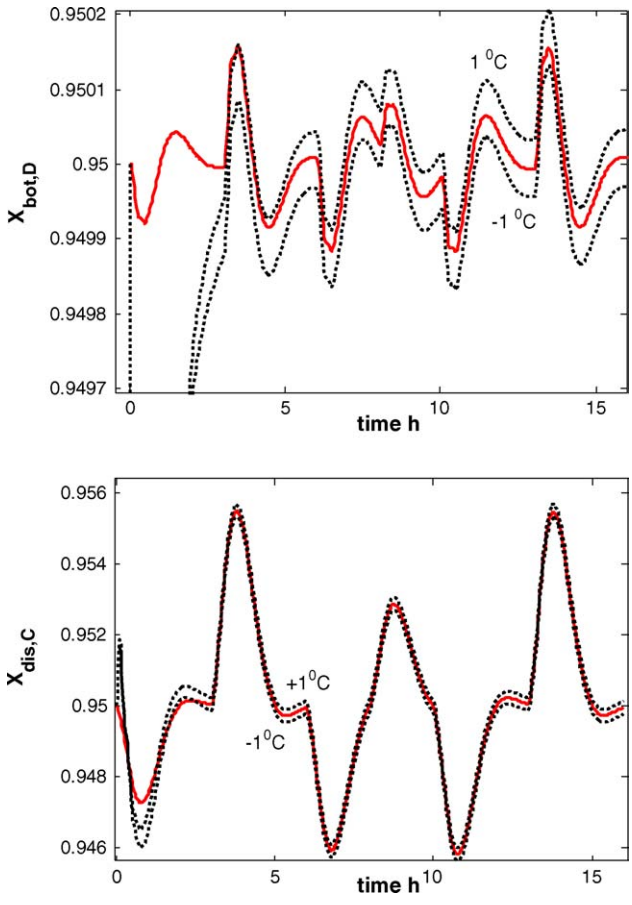

Fig. 11. Control performance in presence $\pm 1\,^{\circ}$C temperature bias on the measurement located on the two feed trays with a PRRS disturbance on F_B: the base initial condition errors, $\delta_m = 10\%$ and $\delta_p = 1\%$ are used for the KF design; (—) measured states for feedback; (- - -) estimated states for feedback.

5.4. Measurement error

In order to investigate the effect of the measurement errors on the state estimator performance, and the impact on the control system as a whole, the temperature bias of the thermocouples in the two feed trays of reactants A and B are changed by $\pm 1\,^{\circ}C$. Fig. 11 demonstrates that an acceptable control performance could still be achieved in spite of the present measurement errors. However, because the measurement errors are deterministic and the controllers are designed to track the setpoint based upon the information on the estimated states, the effect of measurement errors on the control performance will always remain. Therefore, minimizing the measurement errors, as much as possible, in the output data supplied to the estimator will provide an overall good control performance.

6. Conclusion

A linearized state space model for a generic reactive distillation has been formulated. The development of the model only requires the information about the steady state design data, including the holdup in all the stages and the stationary composition profiles in the column. The linearity of the model is attested by the uniform and symmetric nature of the output responses to different magnitudes of step inputs.

The application of a linear state estimator in a model-based control of a reactive distillation using the linearized process model is explored. It is demonstrated that a robust linear estimator can be successfully implemented in a feedback system of a linear reactive distillation provided that a reliable approximate process model can be obtained. It is shown that a well-tuned controller gains are a necessity for a good performance of estimator-based control system of reactive distillation. The robustness of the estimator-based control system is explored when a state estimator is designed from the erroneous initial conditions, measurement errors and erroneous noise plant model. Some of our future work will focus on dynamic comparison of the linear and the nonlinear models.

Acknowledgement

The authors acknowledge King Fahd University of Petroleum and Minerals, Dhahran, Saudi Arabia, for supporting this research.

References

Al-Arfaj, M. A., & Luyben, W. L. (2000). Comparison of alternative control structures for an ideal two-product reactive distillation column. *Industrial & Engineering Chemistry Research*, *39*, 3298–3307.

Al-Arfaj, M. A., & Luyben, W. L. (2002a). Comparative control study of ideal and methyl acetate reactive distillation. *Chemical Engineering Science*, *24*(57), 5039–5050.

Al-Arfaj, M. A., & Luyben, W. L. (2002b). Control study of ethyl *tert*-butyl ether reactive distillation. *Industrial & Engineering Chemistry Research*, *41*, 3784–3796.

Al-Arfaj, M. A., & Luyben, W. L. (2004). Plantwide control for TAME production using reactive distillation. *American Institute of Chemical Engineers Journal*, *50*(7), 1462–1473.

Baur, R., Taylor, R., & Krishna, R. (2001). Dynamic behavior of reactive distillation tray columns described with a nonequilibrium cell model. *Chemical Engineering Science*, *56*, 1721–1729.

Bisowarno, B. H., Tian, Y.-C., & Tade, M. O. (2003). Model gain scheduling control of an ethyl *tert*-butyl ether reactive distillation column. *Industrial & Engineering Chemistry Research*, *42*, 3584–3591.

Chen, C.-T. (1999). *Linear system theory and design*. New York: Oxford University Press.

Kumar, A., & Daoutidis, P. (1999). Modeling, analysis and control of an ethylene glycol reactive distillation column. *American Institute of Chemical Engineers Journal*, 45–51.

Luyben, W. L. (1987). Derivation of transfer functions for highly nonlinear distillation columns. *Industrial & Engineering Chemistry Research*, *26*, 2490–2495.

Luyben, W. L. (2000). Economic and dynamic impact of the use of excess reactant in reactive distillation systems. *Industrial & Engineering Chemistry Research*, *39*, 2935–2946.

Marquardt, W., & Amrhein, M. (1994). Development of a linear distillation model from design data for process control. *Computers & Chemical Engineering*, *18*, S349–S353.

Roat, S., Downs, J. J., Vogel, E. F., & Doss, J. E. (1986). Integration of rigorous dynamic modeling and control system synthesis for distillation columns. *Chemical Process Controls CPC III* (pp. 99–138). Amsterdam, The Netherlands: Elsevier.

Sorenson, H. W. (Ed.). (1985). *Kalman filtering: Theory and application*. New York: IEEE Press.

Taylor, R., & Krishna, R. (2000). Modeling reactive distillation. *Chemical Engineering Science*, *55*, 5183–5229.

Tyreus, B. D., & Luyben, W. L. (1992). Tuning PI controllers for integrator/dead time processes. *Industrial & Engineering Chemistry Research*, *31*, 2625–2628.

Wang, S., Wong, D. S. H., & Lee, E. (2003). Control of a reactive distillation column in the kinetic regime for the synthesis of *n*-butyl acetate. *Industrial & Engineering Chemistry Research*, *42*, 5182–5194.

Wolbert, D., Joulia, X., Koehret, B., & Biegler, L. T. (1994). Flowsheet optimization and optimal sensitivity analysis using analytical derivatives. *Computers & Chemical Engineering*, *18*, 1083–1095.